

Cite this: *Chem. Commun.*, 2018, 54, 10060Received 9th May 2018,  
Accepted 12th July 2018

DOI: 10.1039/c8cc03744b

rsc.li/chemcomm

**Two poly-oxo cluster complexes of tetravalent neptunium (Np(IV)),  $\text{Np}_{38}\text{O}_{56}\text{Cl}_{18}(\text{bz})_{24}(\text{THF})_8 \cdot n\text{THF}$  and  $\text{Np}_{38}\text{O}_{56}\text{Cl}_{42}(\text{ipa})_{20} \cdot m\text{ipa}$  (bz = benzoate, THF = tetrahydrofuran, and ipa = isopropanol), were obtained via solvothermal synthesis and structurally characterised by single-crystal X-ray diffraction. The  $\{\text{Np}_{38}\}$  clusters are comparable to the analogous  $\{\text{U}_{38}\}$  and  $\{\text{Pu}_{38}\}$  motifs, filling the gap in this largest poly-oxo cluster series of tetravalent actinides.**

Owing to its diversity as well as its technological importance in the nuclear industry, the polymer and cluster chemistry of actinides (An) has been flourishing since the last decade.<sup>1–5</sup> In particular, the poly-oxo/hydroxo polymer and cluster complexes of tetravalent actinides (An(IV)) have received considerable attention,<sup>6–20</sup> as the formation of these complexes stems primarily from their hydrolysis<sup>21–24</sup> and, hence, it would have significant implications for the natural and engineered aqueous systems associated with the nuclear industry.<sup>25</sup> The largest poly-oxo An(IV) cluster reported thus far is the  $\{\text{An}_{38}\}$  complex, consisting of 38 An(IV) centres bridged by 56 oxygens. This type of cluster complex has been synthesised and characterised for U(IV)<sup>9,26</sup> and Pu(IV),<sup>13,15</sup> and this cluster motif could be stable in solution in a colloidal form.<sup>13,15,27</sup> In the periodic table, neptunium ( $_{93}\text{Np}$ ) is present between  $_{92}\text{U}$  and  $_{94}\text{Pu}$ . Despite its importance in nuclear fuel reprocessing and radioactive waste management,<sup>25</sup> the research on Np always lags behind those on U and Pu,<sup>28</sup> which is also the case for the chemistry of poly-oxo/hydroxo polymers and clusters. In order to fill the gap between the  $\{\text{U}_{38}\}$  and  $\{\text{Pu}_{38}\}$  clusters and to complete a series of these largest poly-oxo An(IV)

## $\{\text{Np}_{38}\}$ clusters: the missing link in the largest poly-oxo cluster series of tetravalent actinides†

Nicolas P. Martin,<sup>a</sup> Christophe Volkringer,<sup>ab</sup> Pascal Roussel,<sup>a</sup> Juliane März,<sup>c</sup> Christoph Hennig,<sup>b</sup> Thierry Loiseau<sup>ib\*</sup> and Atsushi Ikeda-Ohno<sup>ib\*†c</sup>

cluster complexes, we report herein the synthesis and characterisation of the first  $\{\text{Np}_{38}\}$  cluster complexes, which are also the largest single molecules of Np reported thus far.

The first  $\{\text{Np}_{38}\}$  complex,  $\text{Np}_{38}\text{O}_{56}\text{Cl}_{18}(\text{bz})_{24}(\text{THF})_8 \cdot n\text{THF}$ † (1, bz = benzoate, THF = tetrahydrofuran), was obtained via solvothermal synthesis with  $\text{NpCl}_4$ , benzoic acid, THF and deionised water (Sections 1 and 2 in the ESI†), which is a slight modification of the synthesis of the  $\{\text{U}_{38}\}$  complex.<sup>9</sup> After 1 day of heating at 400 K, purple/brown crystals with an octahedral shape were deposited (Fig. 1, left). Single-crystal X-ray diffraction (SC-XRD) measurements on the obtained crystals reveal the discrete  $\{\text{Np}_{38}\}$  motif shown in Fig. 2a. The second  $\{\text{Np}_{38}\}$  complex,  $\text{Np}_{38}\text{O}_{56}\text{Cl}_{42}(\text{ipa})_{20} \cdot m\text{ipa}$ † (2, ipa = isopropanol), was synthesised solvothermally from a mixture of  $\text{NpCl}_4$  and benzoic acid in isopropanol (Sections 1–3 in the ESI†). Heating the sample mixture at 370 K for 3 days resulted in the formation of purple/brown crystals with an octahedral shape (Fig. 1, right). The complex structure determined by SC-XRD shows another  $\{\text{Np}_{38}\}$  motif, as illustrated in Fig. 2b.

Both compounds 1 and 2 crystallise in the tetragonal space group  $I4/m$  (Table S1 in the ESI†), which is the same as that observed for the analogous  $\{\text{U}_{38}\}$  clusters  $\text{U}_{38}\text{O}_{56}\text{Cl}_{18}(\text{bz})_{24}(\text{THF})_8 \cdot 8\text{THF}$ <sup>9</sup> and  $\text{U}_{38}\text{O}_{56}\text{Cl}_{42}(\text{H}_2\text{O})_2(\text{ipa})_{20} \cdot x\text{ipa}$ .<sup>26</sup> Both the  $\{\text{Np}_{38}\}$  clusters are composed of a  $\{\text{Np}_{14}\}$  core (light green polyhedra in Fig. 2) surrounded by six tetranuclear  $\{\text{Np}_4\}$  subunits (blue and dark

<sup>a</sup> Unité de Catalyse et Chimie du Solide (UCCS), UMR, CNRS 8181, Université de Lille, École Nationale Supérieure de Chimie de Lille Centrale Lille, Université Artois, Lille 59000, France. E-mail: thierry.loiseau@ensc-lille.fr

<sup>b</sup> Institut Universitaire de France, 1 rue Descartes, Paris Cedex 05 75231, France

<sup>c</sup> Helmholtz-Zentrum Dresden-Rossendorf (HZDR), Institute of Resource Ecology, Bautzner Landstraße 400, Dresden 01328, Germany. E-mail: a.ikeda@hzdr.de

† Electronic supplementary information (ESI) available: Synthetic details, crystal structure determination and interpretation, discussions on tetranuclear complexes, and crystallographic data. CCDC 1840373 and 1840572. For ESI and crystallographic data in CIF or other electronic format see DOI: 10.1039/c8cc03744b



Fig. 1 Optical micrographs of single crystals of the  $\{\text{Np}_{38}\}$  compounds synthesised from THF (1, left) and isopropanol (2, right).



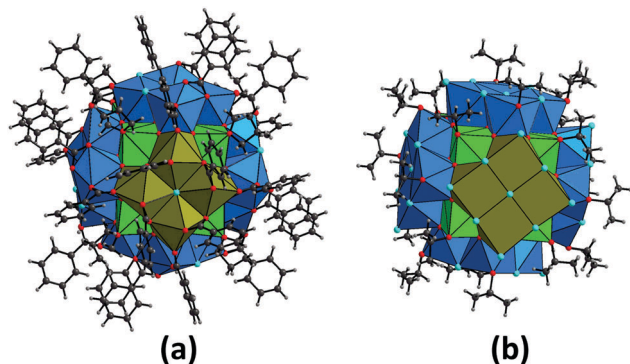


Fig. 2 Molecular structures of the two  $\{Np_{38}\}$  clusters  $Np_{38}O_{56}Cl_{18}(bz)_{24}(THF)_8$  (**1**, a) and  $Np_{38}O_{56}Cl_{42}(ipa)_{20}$  (**2**, b).§ The coordination geometry around neptunium atoms (as  $Np^{4+}$ ) is illustrated with coloured polyhedra, whilst carbon (black), chlorine (light blue), hydrogen (grey) and oxygen (red) atoms are shown as balls. The cubic  $\{Np_{14}\}$  cores are depicted with light green, whilst the exterior  $\{Np_4\}^{tetra}$  and  $\{Np_4\}^m$  subunits adhering to the  $\{Np_{14}\}$  core are illustrated with blue and dark brown, respectively.

brown polyhedra in Fig. 2). In the  $\{Np_{14}\}$  core, three crystallographically distinct Np atoms (Np1, Np2 and Np3) are packed in a dense manner, forming a primitive unit of the fluorite structure (Fig. S1 in the ESI†) which is the basis of bulk  $NpO_2$ .<sup>29,30</sup> The eight corners of the cubic  $\{Np_{14}\}$  core are all occupied by the oxygen atoms of THF- or isopropanol molecules for **1** and **2**, respectively (Fig. S1 in the ESI†). Each face of the cubic  $\{Np_{14}\}$  core is further decorated with the  $\{Np_4\}$  subunits, where there is a significant difference between **1** and **2**. In both the  $\{Np_{38}\}$  compounds, two types of  $\{Np_4\}$  subunits appear. The first type (referred to as “ $\{Np_4\}^{tetra}$ ” hereafter) appears four times by symmetry operation with respect to the tetragonal axis, whilst the second type (referred to as “ $\{Np_4\}^m$ ” hereafter) appears twice around the  $\{Np_{14}\}$  core as a result of the perpendicular mirror plane operation. The coordination polyhedra of the Np atoms in the inner  $\{Np_{14}\}$  core are cubic, whilst those in the exterior  $\{Np_4\}$  subunits are square antiprismatic polyhedra (Fig. 3). This results in two different types of oxo-bridging groups in the  $\{Np_{38}\}$  clusters;  $\mu_4$ -O with Np–O distances of 2.294(9)–2.408(9) and 2.28(4)–2.42(4) Å for **1** and **2**, respectively, and  $\mu_3$ -O with Np–O distances of 2.203(9)–2.335(10) and 2.15(4)–2.305(3) Å for **1** and **2**, respectively. These Np–O distances are comparable to those in the fluorite-based  $NpO_2$  structure (2.353–2.354 Å),<sup>29,30</sup> suggesting that the Np–O framework in the  $\{Np_{38}\}$  clusters could also be comparable to that in the bulk  $NpO_2$ .

In compound **1**, the  $\{Np_4\}^{tetra}$  subunit (blue polyhedra in Fig. 2a and 3a) is composed of three distinct Np centres (Np4, Np5 and Np6). The four Np atoms are linked *via* either  $\mu_2/\mu_4$ -Cl atoms or bidentately coordinating the carboxylate groups of bz, forming a ninefold coordination geometry with distorted trideca- and undecahedra around Np4 and Np5, respectively, and an eightfold geometry with a distorted nonahedron around Np6 (Fig. 3a). Each  $\{Np_4\}^{tetra}$  subunit adheres to one side of the cubic  $\{Np_{14}\}$  core *via* twelve O atoms facing the core, covering the four sides of the  $\{Np_{14}\}$  cube. On the other hand, the  $\{Np_4\}^m$  subunit (dark brown polyhedra in Fig. 2a and 3b) is composed of a single type of a distinct Np centre (Np7). The four Np atoms in the



Fig. 3 Top-side views of the  $\{Np_4\}$  subunits in **1** and **2**; the  $\{Np_4\}^{tetra}$  and  $\{Np_4\}^m$  subunits in **1** (a and b, respectively) and those in **2** (c and d, respectively).§ All these subunits contain unique  $\mu_4$ -bridging Cl atoms. The coordination geometry around neptunium atoms (as  $Np^{4+}$ ) is illustrated with blue and dark brown polyhedra ( $\{Np_4\}^{tetra}$  and  $\{Np_4\}^m$ , respectively), whilst carbon (black), chlorine (light blue), hydrogen (grey) and oxygen (red) atoms are shown as balls.

$\{Np_4\}^m$  subunit are linked *via* one  $\mu_4$ -Cl atom and four carboxylate groups of bz, forming a ninefold coordination geometry with a dodecahedron around the Np7 atoms (Fig. 3b). This  $\{Np_4\}^m$  subunit covered the rest of the two sides of the  $\{Np_{14}\}$  cube, and is further connected with the  $\{Np_4\}^{tetra}$  subunit by the bidentate carboxylate groups of bz to overlay the  $\{Np_{14}\}$  core (Fig. 2a).

Despite the presence of benzoic acid in the initial sample solution, no benzoate groups are involved in the formation of the  $\{Np_{38}\}$  cluster in **2**, which is in contrast to **1**. The exterior  $\{Np_4\}$  subunits in **2** are composed of the O atoms of isopropanol molecules, Cl<sup>−</sup> ions and the O<sub>oxo</sub> groups shared with the  $\{Np_{14}\}$  core. The  $\{Np_4\}^{tetra}$  subunit in **2** is composed of three distinct Np centres (Np4, Np5 and Np6), all of which form an eightfold square antiprismatic geometry (Fig. 3c). In the  $\{Np_4\}^m$  subunit of **2**, there is only a single distinct Np centre (Np7) which is surrounded by four O<sub>oxo</sub> groups shared with the  $\{Np_{14}\}$  core and four Cl<sup>−</sup> ions, eventually forming an eightfold square antiprismatic geometry as well (Fig. 3d). In a similar manner to the arrangement in **1**, the six  $\{Np_4\}$  subunits decorate the exterior of the cubic  $\{Np_{14}\}$  core to form an  $\{Np_{38}\}$  cluster.

The chemical formulae of  $[Np_{38}O_{56}Cl_{18}(bz)_{24}(THF)_8]$  (**1**) and  $[Np_{38}O_{56}Cl_{42}(ipa)_{20}]$  (**2**) derived from SC-XRD both exhibit an excess negative charge of  $-2$ , assuming that the Np atoms in the clusters are all tetravalent (*i.e.*  $Np^{4+}$ ). No cationic species are identified in the crystal packing of **1** and **2** either, indicating that the  $\{Np_{38}\}$  cluster units should be neutral. This discrepancy can be, however, explained by the partial replacement of chloride anions (Cl<sup>−</sup>) with neutral water molecules (H<sub>2</sub>O) in the  $\{Np_4\}$  subunits and/or the replacement of the  $\mu_3$ -oxo groups with the hydroxo ones in the inner  $\{Np_{14}\}$  core. Further detailed discussions are provided in the ESI† (Section 3).



Albeit a series of  $\{\text{An}_{38}\}$  clusters (*i.e.*  $\{\text{U}_{38}\}$ ,<sup>9,26</sup>  $\{\text{Np}_{38}\}$  in this study, and  $\{\text{Pu}_{38}\}$ <sup>13,15</sup>) were successfully characterised, their formation mechanism has been unrevealed even to date. All the  $\{\text{An}_{38}\}$  clusters characterised thus far are composed of an inner  $\{\text{An}_{14}\}$  core decorated with six exterior  $\{\text{An}_4\}$  subunits. Given this construction manner, it is reasonable to infer that the formation of the primary  $\{\text{An}_{14}\}$  core is followed by the attachment of the  $\{\text{An}_4\}$  subunits to the surface of the cubic  $\{\text{An}_{14}\}$  core. Owing to their strong ololation/oxolation tendency,<sup>31</sup> An(IV) can form a variety of oligomer species<sup>2</sup> including soluble  $\mu_2$ -hydroxo-bridged dinuclear species,<sup>7,17,32</sup> which could further evolve into hexanuclear species *via* hydrolysis.<sup>6,10,11,14</sup> A similar evolution of such oligomer species was also observed for Ce(IV),<sup>33,34</sup> a chemical analogue of An(IV). The union of di- and hexanuclear species could also lead to the formation of  $\{\text{An}_{12}\}$  complexes.<sup>8</sup> However, to the best of our knowledge, no  $\{\text{An}_{14}\}$  complexes have been characterised for An(IV) thus far, indicating that the  $\{\text{An}_{14}\}$  motif is probably not stable at least as a discrete species. In contrast, several discrete  $\{\text{An}_4\}$  complexes have been characterised for Th(IV)<sup>35</sup> and U(IV),<sup>36–43</sup> seven of which exhibit a planar tetranuclear arrangement that is structurally comparable with the  $\{\text{An}_4\}$  subunits in the  $\{\text{An}_{38}\}$  clusters (Section 4 in the ESI†). A striking difference between the  $\{\text{An}_4\}$  subunits and the discrete tetranuclear An(IV) complexes is, however, the presence/absence of  $\mu_4$ -bridging groups. As illustrated in Fig. 3, there are unique  $\mu_4$ -bridging Cl atoms situated at the centre of the  $\{\text{Np}_4\}$  subunits, which are observed for the whole series of  $\{\text{An}_{38}\}$  clusters. On the other hand, none of the discrete tetranuclear An(IV) complexes contains  $\mu_4$ -bridging groups (Table S2 and Fig. S2 in the ESI†), except one Th(IV) complex<sup>35</sup> containing a  $\mu_4$ -bridging oxo group to form a unique non-planar boat conformation arrangement (Fig. S3 in the ESI†). Instead, these discrete tetranuclear complexes are composed of  $\mu_2$ - and  $\mu_3$ -bridging groups (Table S2 and Fig. S3 in the ESI†), suggesting that the planar  $\{\text{An}_4\}$  motif with a  $\mu_4$ -bridging group may also not be stable as a discrete species. Given all these facts, the formation process of the  $\{\text{An}_{38}\}$  clusters could be surmised as follows:

(1) the primitive but transient  $\{\text{An}_{14}\}$  core is formed *via* the ololation/oxolation of precursor species (*e.g.* dinuclear and/or hexanuclear species),

(2) owing to an extremely large negative charge of the primitive  $\{\text{An}_{14}\}$  core ( $-72$  based on the formula  $\text{An}_{14}\text{O}_{64}$  (Fig. S1 in the ESI†)), cationic species in the system (*i.e.*  $\text{An}^{4+}$ ) are further attracted to the surface of the  $\{\text{An}_{14}\}$  core immediately after the formation of the primitive core, forming dense  $\{\text{An}_4\}$  subunits containing  $\mu_4$ -bridging groups on the surface, and

(3) the attachment of six  $\{\text{An}_4\}$  subunits on each face of the cubic  $\{\text{An}_{14}\}$  core neutralises the negative charge of the  $\{\text{An}_{14}\}$  core, eventually stabilising the whole unit as  $\{\text{An}_{38}\}$ .

Based on this hypothetical formation process, it is obvious that the faces of the primitive  $\{\text{An}_{14}\}$  core provide a sort of “substrate” for the formation of unique planar  $\mu_4$ -bridged  $\{\text{An}_4\}$  subunits. In other words, such a planar  $\mu_4$ -bridged  $\{\text{An}_4\}$  motif could be formed and stabilised only when an appropriate substrate exists in the system.

As previously mentioned, the inner  $\{\text{An}_{14}\}$  core in the  $\{\text{An}_{38}\}$  cluster is a primitive unit of the fluorite-based  $\text{AnO}_2$  structure.

The  $\{\text{An}_4\}$  subunits in the cluster also show a closer structural conformity to the bulk  $\text{AnO}_2$  structure as compared with the discrete tetranuclear An(IV) complexes (Fig. S4 in Section 4, ESI†). All these facts indicate that the poly-oxo  $\{\text{An}_{38}\}$  clusters can be the origin of the formation of  $\text{AnO}_2$  in solution. As a matter of fact, the  $\{\text{An}_{38}\}$  clusters can easily evolve into bulk  $\text{AnO}_2$  by moderate hydrolysis.<sup>9,26</sup> Given the electroneutrality of the  $\{\text{An}_{38}\}$  clusters, the  $\{\text{An}_{38}\}$  motif will no longer attract additional metal cations (*i.e.*  $\text{An}^{4+}$ ) to form larger clusters. Hence, the  $\{\text{An}_{38}\}$  unit is probably the largest poly-oxo An(IV) cluster stabilised in solution, which is also the limiting point that defines the border between discrete poly-oxo oligomer/cluster complexes and insoluble bulk  $\text{AnO}_2$ , including colloidal species or aggregates.

In summary, this study succeeded in synthesising and structurally characterising the two poly-oxo Np(IV) cluster complexes **1** and **2** which are composed of 38 Np atoms. The characterised  $\{\text{Np}_{38}\}$  clusters are the largest discrete Np complexes reported thus far, filling the gap between the already reported  $\{\text{U}_{38}\}$  and  $\{\text{Pu}_{38}\}$  clusters to complete a series of  $\{\text{An}_{38}\}$  cluster complexes. Although hexavalent An cations (as actinyl(VI) cations:  $\text{AnO}_2^{2+}$ ) can form poly-oxo clusters larger than 100-mer based on the cage structure which is not directly comparable with open clusters,<sup>3</sup> the  $\{\text{An}_{38}\}$  motif is probably the largest open cluster unit for the poly-oxo An(IV) complexes that can be stabilised as a discrete species in solution. A series of poly-oxo  $\{\text{An}_{38}\}$  clusters (An = U, Np and Pu) exhibits a significant structural similarity, suggesting a similar ololation/oxolation (*i.e.* hydrolysis) behaviour amongst these lighter An(IV) series. A comparison of the series of  $\{\text{An}_{38}\}$  clusters with the large poly-oxo clusters of other metals (*e.g.*  $\text{Ti}^{4+}$  or  $\text{Bi}^{45}$ ) will further highlight the peculiarity or generality of the chemistry of An(IV) on the periodic table, particularly in terms of hydrolysis and coordination chemistry.

The authors acknowledge the financial support from TALISMAN (Project ID: TALI\_C05-18) and the German Academic Exchange Service (DAAD, Project No 57314018).

## Conflicts of interest

There are no conflicts to declare.

## Notes and references

‡ The Fourier maps of electronic density residues on the collected SC-XRD data show diffused peaks in the void between the  $\{\text{Np}_{38}\}$  units. These peaks probably correspond to neutral solvent molecules (*i.e.* THF in **1** and isopropanol in **2**) intercalated in the crystal structures, as observed in the analogous  $\{\text{U}_{38}\}$  compounds.<sup>9,26</sup> However, owing to the limited quality of the collected SC-XRD data, it is difficult to determine the positions of these intercalated solvent molecules. For this reason, the number of solvent molecules is not specified in the chemical formulae of **1** and **2**.

§ The carbon atoms of some benzoate (bz) molecules in **1** show disorder, statistically populating at two close sites with equivalent occupancy. This disorder is, however, not illustrated in Fig. 2a and 3a for clarity.

- 1 S. Hickam and P. C. Burns, in *Recent Development in Clusters of Rare Earths and Actinides: Chemistry and Materials*, ed. Z. Zheng, Springer-Verlag, Berlin, Heidelberg, 2017, vol. 173, pp. 121–153.
- 2 K. E. Knope and L. Soderholm, *Chem. Rev.*, 2013, **113**, 944–994.
- 3 J. Qiu and P. C. Burns, *Chem. Rev.*, 2013, **113**, 1097–1120.
- 4 T. Loiseau, I. Mihalcea, N. Henry and C. Volkringer, *Coord. Chem. Rev.*, 2014, **266–267**, 69–109.



- 5 W. Yang, T. G. Parker and Z.-M. Sun, *Coord. Chem. Rev.*, 2015, **303**, 86–109.
- 6 C. Tamain, T. Dumas, C. Hennig and P. Guilbaud, *Chem. – Eur. J.*, 2017, **23**, 6864–6875.
- 7 K. E. Knope, S. Skanthakumar and L. Soderholm, *Inorg. Chem.*, 2015, **54**, 10192–10196.
- 8 C. Falaise, C. Volkringer, C. Hennig and T. Loiseau, *Chem. – Eur. J.*, 2015, **21**, 16654–16664.
- 9 C. Falaise, C. Volkringer, J. F. Vigier, A. Beaurain, P. Roussel, P. Rabu and T. Loiseau, *J. Am. Chem. Soc.*, 2013, **135**, 15678–15681.
- 10 K. E. Knope and L. Soderholm, *Inorg. Chem.*, 2013, **52**, 6770–6772.
- 11 K. Takao, S. Takao, A. C. Scheinost, G. Bernhard and C. Hennig, *Inorg. Chem.*, 2012, **51**, 1336–1344.
- 12 B. Biswas, V. Mougél, J. Pecaut and M. Mazzanti, *Angew. Chem., Int. Ed.*, 2011, **50**, 5745–5748.
- 13 R. E. Wilson, S. Skanthakumar and L. Soderholm, *Angew. Chem., Int. Ed.*, 2011, **50**, 11234–11237.
- 14 S. Takao, K. Takao, W. Kraus, F. Emmerling, A. C. Scheinost, G. Bernhard and C. Hennig, *Eur. J. Inorg. Chem.*, 2009, 4771–4775.
- 15 L. Soderholm, P. M. Almond, S. Skanthakumar, R. E. Wilson and P. C. Burns, *Angew. Chem., Int. Ed.*, 2008, **47**, 298–302.
- 16 G. Nocton, F. Burdet, J. Pécaut and M. Mazzanti, *Angew. Chem., Int. Ed.*, 2007, **46**, 7574–7578.
- 17 R. E. Wilson, S. Skanthakumar, G. Sigmon, P. C. Burns and L. Soderholm, *Inorg. Chem.*, 2007, **46**, 2368–2372.
- 18 J. C. Berthet, P. Thuery and M. Ephritikhine, *Chem. Commun.*, 2005, 3415–3417.
- 19 L. M. Mokry, N. S. Dean and C. J. Carrano, *Angew. Chem., Int. Ed.*, 1996, **35**, 1497–1498.
- 20 D. W. Wester, *Inorg. Chem.*, 1982, **21**, 3382–3385.
- 21 *Chemical Thermodynamics of Thorium*, OECD Nuclear Energy Agency, Paris, France, 2007.
- 22 I. Grenthe, J. Fuger, R. J. M. Konings, R. J. Lemire, A. B. Muller, C. Nguyen-Trung Cregu and H. Wanner, *Chemical Thermodynamics of Uranium*, OECD-NEA, Paris, France, 2004.
- 23 R. Guillaumont, T. Fanghänel, J. Fuger, I. Grenthe, V. Neck, D. A. Palmer and M. H. Rand, *Update on the Chemical Thermodynamics of Uranium, Neptunium, Plutonium, Americium and Technetium*, Elsevier, Amsterdam, the Netherlands, 2003.
- 24 R. J. Lemire, J. Fuger, S. Spahiu, J. C. Sullivan, H. Nitsche, W. J. Ullman, P. Potter, P. Vitorge, M. H. Rand, H. Wanner and J. Rydberg, *Chemical Thermodynamics of Neptunium and Plutonium*, Elsevier, Amsterdam, the Netherlands, 2001.
- 25 *The Chemistry of the Actinide and Transactinide Elements*, 4th edn, Springer, The Netherlands, 2011.
- 26 N. P. Martin, C. Volkringer, N. Henry, X. Trivelli, G. Stoclet, A. Ikeda-Ohno and T. Loiseau, *Chem. Sci.*, 2018, **9**, 5021–5032.
- 27 C. Walther and M. A. Denecke, *Chem. Rev.*, 2013, **113**, 995–1015.
- 28 J. Ibers, *Nat. Chem.*, 2010, **2**, 996.
- 29 L. B. Asprey, F. H. Ellinger, S. Fried and W. H. Zacharlasen, *J. Am. Chem. Soc.*, 1955, **77**, 1707.
- 30 W. H. Zacharlasen, *Acta Crystallogr.*, 1949, **2**, 388–390.
- 31 M. Henry, J. P. Jolivet and J. Livage, *Struct. Bonding*, 1992, **77**, 153–206.
- 32 G. Johansson, *Acta Chem. Scand.*, 1968, **22**, 399–409.
- 33 C. Hennig, A. Ikeda-Ohno, W. Kraus, S. Weiss, P. Pattison, H. Emerich, P. M. Abdala and A. C. Scheinost, *Inorg. Chem.*, 2013, **52**, 11734–11743.
- 34 A. Ikeda-Ohno, S. Tsushima, C. Hennig, T. Yaita and G. Bernhard, *Dalton Trans.*, 2012, **41**, 7190–7192.
- 35 N. E. Travia, B. L. Scott and J. L. Kiplinger, *Chem. – Eur. J.*, 2014, **20**, 16846–16852.
- 36 C. Falaise, C. Volkringer and T. Loiseau, *Cryst. Growth Des.*, 2013, **13**, 3225–3231.
- 37 J. D. Rinehart, S. A. Kozimor and J. R. Long, *Angew. Chem., Int. Ed.*, 2010, **49**, 2560–2564.
- 38 L. Salmon, P. Thuéry and M. Ephritikhine, *Polyhedron*, 2006, **25**, 1537–1542.
- 39 J. Rebizant, M. R. Spirlet and C. Apostolidis, *Acta Crystallogr.*, 1992, **C48**, 452–454.
- 40 A. Domingos, N. Marques, A. Pires De Matos, I. Santos and M. Silva, *Polyhedron*, 1992, **11**, 2021–2025.
- 41 P. Charpin, G. Folcher, M. Nierlich, M. Lance, D. Vigner, A. Navaza and C. De Rango, *Acta Crystallogr.*, 1990, **C46**, 1778–1781.
- 42 N. Brianese, U. Casellato, F. Ossola, M. Porchia, G. Rossetto and P. Zanella, *J. Organomet. Chem.*, 1989, **365**, 223–232.
- 43 F. Calderazzo, G. Dell'Amico, M. Pasquali and G. Perego, *Inorg. Chem.*, 1978, **17**, 474–479.
- 44 M. Y. Gao, F. Wang, Z. G. Gu, D. X. Zhang, L. Zhang and J. Zhang, *J. Am. Chem. Soc.*, 2016, **138**, 2556–2559.
- 45 P. C. Andrews, G. B. Deacon, C. M. Forsyth, P. C. Junk, I. Kumar and M. Maguire, *Angew. Chem., Int. Ed.*, 2006, **45**, 5638–5642.

